

Contribution of vacancies to relaxation in amorphous materials: A kinetic activation-relaxation technique study

Jean-Francois Joly,¹ Laurent Karim Béland,¹ Peter Brommer,^{1,2} and Normand Mousseau¹

¹*Département de Physique and Regroupement Québécois sur les Matériaux de Pointe, Université de Montréal, C.P. 6128, Succursale Centre-Ville, Montréal, H3C 3J7, Québec, Canada*

²*Department of Physics and Centre for Scientific Computing, University of Warwick, Coventry CV5 7AL, United Kingdom*

(Received 18 December 2012; published 30 April 2013)

The nature of structural relaxation in disordered systems such as amorphous silicon (*a*-Si) remains a fundamental issue in our attempts at understanding these materials. While a number of experiments suggest that mechanisms similar to those observed in crystals, such as vacancies, could dominate the relaxation, theoretical arguments point rather to the possibility of more diverse pathways. Using the kinetic activation-relaxation technique, an off-lattice kinetic Monte Carlo method with on-the-fly catalog construction, we resolve this question by following 1000 independent vacancies in a well-relaxed *a*-Si model at 300 K over a timescale of up to one second. Less than one percent of these survive over this period of time and none diffuse more than once, showing that relaxation and diffusion mechanisms in disordered systems are fundamentally different from those in the crystal.

DOI: [10.1103/PhysRevB.87.144204](https://doi.org/10.1103/PhysRevB.87.144204)

PACS number(s): 61.43.Dq, 66.30.-h, 81.40.Ef, 82.20.Db

I. INTRODUCTION

The nature of the microscopic mechanism leading to the structural evolution of disordered solids such as amorphous silicon (*a*-Si) remain controversial for lack of direct evidence. What type of mechanism, for example, is responsible for the heat released during relaxation?^{1–4} Is it a global reorganization of the amorphous network or specific atomistic moves such as the annihilation of localized point defects as suggested by a number of experiments?^{1,5–10}

Amorphous silicon is believed to be a close physical realization of the continuous random network model (CRN) proposed by Zachariassen.¹¹ In the CRN, all atoms are fully coordinated, with a local environment close to that of its crystalline counterpart. It is therefore tempting to argue that, as in crystals, vacancylike point defects can exist, particularly in well-relaxed samples, and play a leading role in their structural evolution. These defects could explain, for instance, the average coordination of about 3.88, significantly below the 4 expected from the CRN, determined by Laaziri *et al.* from high-precision diffraction experiments on pure *a*-Si samples.⁵ It also supports calorimetry experiments that show strong similarities between energy relaxation in *a*-Si and interstitial-vacancy recombination in crystalline silicon (*c*-Si)¹ as well as diffusion and solubility measurements of impurities in *a*-Si,^{6,7,12} which are shown to be heavily influenced by the state of relaxation. The presence of point defects is also compatible with the lower enthalpy observed for the ion-beam enhanced diffusion. This behavior inhibits trapping of the impurities and can be interpreted as the effect of highly mobile ion-beam-generated defects recombining with the less mobile trapping defects.^{9,10}

While the experimental evidence for the importance of point defects in structural relaxation of amorphous materials is considerable, there are good thermodynamical objections to their crucial role. Contrary to the crystalline state, the disordered nature of the CRN allows more localized defects such as isolated floating and dangling bonds.¹³ In this language, a vacancy can be considered as a correlated cluster of undercoordinated atoms, and therefore a state of low entropy.

The question is therefore whether or not a potential elastic energy gain obtained by forming a point defect would be sufficient to overcome the entropy loss.

Because of its fundamental interest, this issue has attracted significant interest over the years. A number of computational studies focused on the short-time stability of vacancies created in 216-atom *a*-Si cells using empirical, tight-binding or *ab initio* molecular dynamics.^{14–18} These groups generally relaxed the vacancy over 1 to 10 ps at temperatures of up to 450 K, before studying their structural and electronic properties at $T = 0$. Most found that the vacancy volume could expand or contract during the energy minimization, depending on the local environment. Miranda *et al.*,¹⁷ however, found that vacancies only showed contraction or complete annihilation, in contradiction with the previous other studies, probably because of the relatively poor statistics of these studies. Urli *et al.*¹⁸ showed, using tight-binding MD, that there was a strong correlation between the Voronoi volume of the atoms neighboring the vacancy site and their charge. Due to the short simulation time available for these studies, no defect diffusion was observed, however, and it was not possible to confirm the role of vacancies in the structural relaxation of *a*-Si, leaving this crucial question open.

To fully establish the role of vacancies in relaxing the amorphous network, it is necessary to perform more extensive simulations. In this article, we use the recently developed kinetic activation-relaxation technique (k-ART), an off-lattice kinetic Monte Carlo method with on-the-fly catalog building to assess vacancy kinetics of a thousand different vacancies run over a time scale of up to one second or more at 300 K. We show, in particular, that vacancies do not diffuse as a whole and that relaxation mechanisms are much richer in amorphous materials than in crystalline solids.

II. METHODS

A. Kinetic ART

Kinetic ART is a parallelized off-lattice kinetic Monte Carlo method (KMC) with on-the-fly catalog building.^{19–22}

It integrates the activation-relaxation technique (ART nouveau), an efficient saddle-point searching method^{23,24} that was used, for example, to characterize the energy landscape of amorphous silicon^{25,26} with the topological graph analysis tool NAUTY.²⁷ Unlike other KMC methods, k-ART uses a topological classification for its events and is therefore not limited to crystalline environments; it can treat with equal ease disordered systems such as *a*-Si, fully taking into account the specific environment around each atom. Local atomic environments are identified by considering a cluster around each atom. The connectivity network (graph) of the cluster is then created using a cutoff distance of 3.0 Å. It is this graph that is sent to NAUTY, which returns a unique topological key. This method of identifying local environments is robust against small changes in distance between neighbors. To generate the catalog, it is assumed that every atom that shares the same topology also shares the same list of activated events.

As explained in more details in Ref. 20, this assumption, for this topological classification, is equivalent to requesting a one-to-one correspondence between the topology and the local geometry. Such correspondence is easily tested since all low-energy saddle points are reconstructed before computing the rate and executing a KMC step. If the saddle point does not exist, we establish that this correspondence does not hold and that more than one geometry corresponds to the same topology. To lift this degeneracy, cutoffs are modified and a new graph is generated in such a way to recover the one-to-one correspondence.

A normal k-ART simulation starts by building a complete catalog of events for each local topology found in the initial configuration. To ensure that the system is well sampled, 50 ART-nouveau searches are launched for each new topology. The atom clusters for the initial, the saddle-point, and the final event configurations are also kept in memory. This way, an entire off-lattice KMC event catalog is built on-the-fly. For the initial search on the full system, an average of 3.3 events were found per atom, in agreement with a previous extensive search of the energy landscape of well-relaxed *a*-Si.²⁶ For a disordered solid such as *a*-Si, most if not all local topologies can be considered unique, requiring a large number of initial ART-nouveau searches. However, most activated events involve only a few tens of atoms moving significantly. This means that once the initial configuration has been thoroughly explored, the subsequent number of event searches needed is much lower. K-ART can therefore be applied efficiently to disordered materials such as amorphous silicon.

Here, the initial k-ART catalog is built using the initial 1000-atom model. The catalog is then simply updated for each of the 1000 defective models derived from this initial configuration. After the catalog is updated, all relevant low-energy transition states, corresponding to at least 99.99% of the rate computed, are fully relaxed to include possible changes in the environment. This is done by mapping the saddle-point configuration of each of these low-barrier events to each atom sharing that same topology and refining the activation barrier. This ensures that long-range elastic effects are taken into account. Following the standard KMC algorithm,²⁸ an event is then selected at random from a Poisson distribution and a move is effected. After this step, a search is made through

all the atoms to identify new topologies and the catalog is updated.

Amorphous systems display a continuous distribution of activated barriers that can start as low as a few meV. Most of these low-energy barriers connect so-called flickers associated with oscillatory states that we handle using a basin acceleration method that directly solves the intrabasin kinetics without having to generate all trajectories.²⁰ A basin of such states is constructed on-the-fly using a predetermined barrier cutoff value. Intrabasin states are only visited once and the exit time associated with the extrabasin transitions is adjusted following the basin autoconstructing mean rate method,²⁰ which extends the mean rate method of Puchala *et al.*²⁹ This ensures that the choice of the basin energy threshold has no impact on the overall kinetics of the system, an important feature for a system with no clear energy cutoff between diffusive and nondiffusive events. In our case, all simulations are started with a basin threshold of 0.3 eV that is manually increased whenever the system is found to be trapped for more than 20 steps.

B. Vacancy models

The initial *a*-Si model used for this work is a high-quality, low-strain 1000-atoms model built using the improved Wooten, Winer, and Weaire (WWW) bond switching method.^{30,31} As was shown by Kim *et al.*,¹⁶ long-range elastic effects can be important when studying vacancies. A 216-atom box can create important distortions, making larger cells essential. We use the modified Stillinger-Weber potential from Vink *et al.*,³² fitted to capture the right structural and vibrational properties of the amorphous phase. Periodic boundary conditions were imposed in all directions and the volume was first optimized to minimize the pressure. Table I shows the structural properties for the initial and relaxed configurations compared with experiments.

One thousand single-vacancy configurations are then created by removing, in turn, every atom from the cell. Each of these 999-atom models is first relaxed into a local energy minimum. All systems for which the vacancy survives are then submitted to a full-fledged k-ART simulation that is pursued until the vacancy disappears or the simulation time reaches a value greater than 0.1 second.

TABLE I. Structural properties of our *a*-Si model vs those of the original WWW model and experimental values. ρ is the density in atoms per Å³; E the total potential energy (eV); $\langle r \rangle$ the average bond length (Å); $\langle \theta \rangle$ the average bond angle (degrees); and $\Delta\theta$ the bond deviation (degrees). The pressure P in GPa and \bar{Z} is the average coordination with a cutoff radius of 2.9 Å.

| Properties | Experiment | Original model | Relaxed model |
|--------------------------|---------------------|----------------|-----------------------|
| ρ | 0.049 ³³ | 0.0521 | 0.0470 |
| E | – | –3012.89 | –3066.78 |
| $\langle r \rangle$ | 2.35 ± 0.001^5 | 2.31 | 2.39 |
| $\langle \theta \rangle$ | 107.83 ± 0.97^5 | 109.17 | 109.24 |
| $\Delta\theta$ | 9.63 ± 0.08^5 | 9.90 | 9.68 |
| P | – | 9.23 | 4.49×10^{-6} |
| \bar{Z} | 3.88 ± 0.01^5 | 4.0 | 4.0 |

The definition of a vacancy in a disordered system is not unique. Here, we focus on the topology of the underlying bond network for identification: A vacancylike defect is defined as a cluster of four threefold coordinated atoms using a cutoff distance of 2.9 Å, situated in the gap between the first- and second-neighbor peak of the radial distribution function (see, for example, Ref. 31). While the specific choice of cutoff affects the quantitative results, we have checked that the qualitative conclusion remains unchanged for any distance within this gap. The free volume associated with the vacancies is calculated, following Kim *et al.*,¹⁶ as $V_{\text{vac}} = \frac{4\pi r_{\text{avg}}^3}{3}$ where r_{avg} is the average distance between the vacancy center and each of its four neighbors. The total stress tensor is computed, following Demkowicz and Argon,³⁴ from the local atomic stress tensor, $(\tau_{ab})_i$ ($a, b = x, y, z$),

$$\tau_{ab} = \frac{1}{N} \sum_{i=1}^N (\tau_{ab})_i, \quad (1)$$

from which we obtain the pressure $P = -\frac{1}{3}\text{tr}(\tau)$. The von Mises stress, σ_{VM} , is also calculated for each atom: $\sigma_{\text{VM}} = \sqrt{3J_2}$, where J_2 is the second invariant of the stress deviator tensor. This quantity provides a picture of the shear stress felt by individual atoms.

A vacancy is considered to have vanished when an activated event results in the partial or total disappearance of the associated coordination defects, without another vacancy being created close by. In some cases, this condition is not sufficient as the local environment oscillates between two states with and without coordination defects. Therefore, to consider the vacancy to have disappeared, we require to observe both a change in coordination and a corresponding energy drop due to the structural relaxation around the defect site. With these criteria, a vacancy in an oscillatory state is therefore considered present in the system.

III. RESULTS

A. Initial relaxation

The change in volume of the vacancy during the initial steepest descent relaxation is strongly correlated with the local pressure felt by the missing atom before it is removed. Figure 1 shows that, as expected, vacancies under compressive stress tend to contract even more while sites under tension also expand by a large amount. In contrast, sites where the atoms are under very little pressure tend to keep their original volume. The original variation of vacancy volumes upon creation is explained simply because sites under compressive (tensile) stress tend to have smaller (longer) bonds, resulting in a smaller (greater) vacancy volume.

The vacancy formation energy, defined as

$$E_f = E_2 - \frac{(N-1)}{N} E_1, \quad (2)$$

where E_1 is the total energy of the full N -atom system and E_2 is the total energy with a single atom removed, represents the work needed to create the vacancy. Figure 2 shows E_f as a function of both the local pressure and atomic von Mises stress. We see that atoms under compression are characterized by a lower formation energy than those under tensile stress

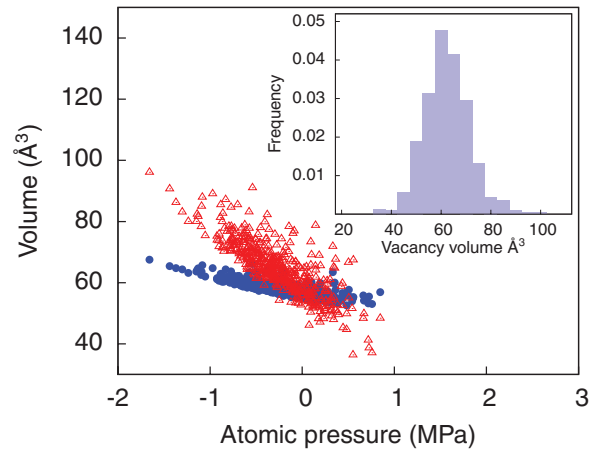


FIG. 1. (Color online) Change in vacancy volumes upon minimization. Volumes of vacancies created from the initial model are in blue and volumes after minimization are in red. Positive pressure is compressive while negative pressure is tensile. Inset: histogram showing the distribution of relaxed volumes for the 453 vacancies surviving relaxation.

and that a high shear stress also reduces the formation energy. E_f is an excellent criterion for predicting the defect stability. All vacancies associated with a formation energy of 1.5 eV or less disappear upon relaxation, leaving at most one or two coordination defects; 93% of the vacancies that disappeared upon minimization had a formation energy under 2.5 eV compared to only 25% of those that survived. Of the original 1000 999-atom models, 547 annihilated their vacancy in this first step, leaving 453 vacancy configurations for k-ART simulations. The final distribution of vacancy volumes (excluding vacancies that were destroyed upon minimization) is shown in the inset of Fig. 1, showing an average volume of $64.9 \pm 9.1 \text{ Å}^3$.

B. k-ART simulations

Kinetic ART simulations were launched on the remaining 453 configurations. As could be expected from disordered systems, their kinetics is dominated by oscillatory events, i.e., flickers, with rare activated mechanisms that lead to effective

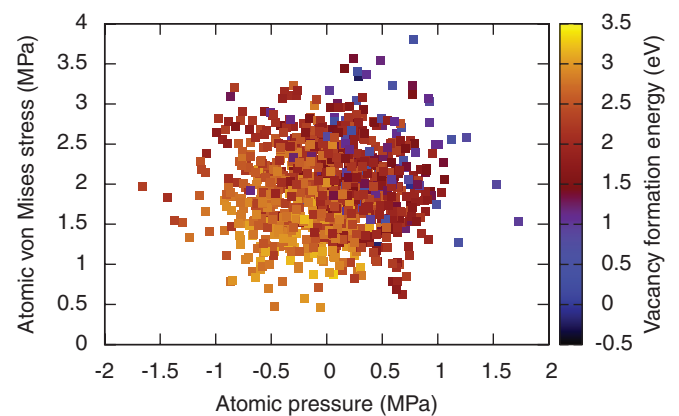


FIG. 2. (Color online) Formation energy (eV) as a function of original atomic pressure and atomic von Mises stress of the atom that was removed.

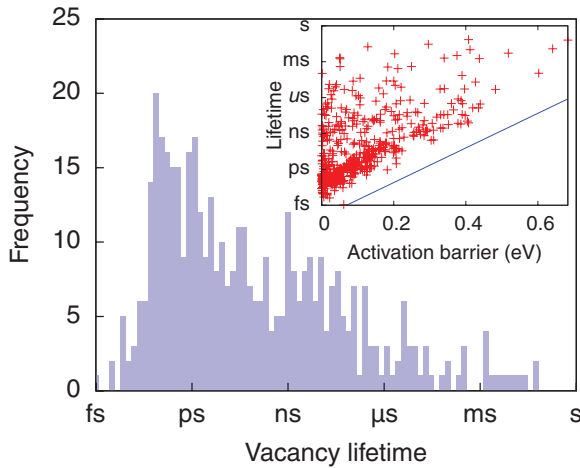


FIG. 3. (Color online) Histogram showing the lifetime of the vacancies that were annihilated. Inset: distribution of lifetimes of stationary vacancies as a function of the activated barrier of the annihilation event (first event where vacancy ceases to be present). The blue line represents the Boltzmann factor at a temperature of 300 K.

structural evolution. The vast majority of vacancies annihilate rapidly—in less than one nanosecond. Figure 3 shows the lifetime distribution of the annihilated vacancies: 175 out of 453 (39%) are unstable and are destroyed after a single k-ART step. The number of surviving vacancies after 1 μ s, 1 ms, and 0.1 s are 43, 13, and 6, respectively. After all simulations were stopped, the remaining six vacancies had been present for 0.12 s (vac 83), 0.14 s (vac 212), 0.17 s (vac 122), 0.19 s (vac 219), 0.36 s (vac 103), and 1.98 s (vac 156). Of these, four were perfectly stable, showing no oscillations or diffusion (vac 83, 156, 212, 122), one (vac 103) was intermittent, and the last one (vac 219) oscillated between two positions. Not surprisingly, all these six surviving vacancies show a large volume, ranging from 73 \AA^3 (vac 103) to 96.4 \AA^3 (vac 156), and are associated, except for vac 103, with a significant local negative pressure that make a local reconstruction much more costly energetically. We see in the inset of Fig. 3 that the lifetime is limited by the activation barrier of the annihilation event with a slope corresponding to a Boltzmann temperature of 300 K. Long lifetimes associated with low-energy barrier indicate that the vacancy annihilation for these systems required a local rearrangement around the vacancy that took place over a number of events.

Diffusion of full vacancies is rare. Only 86 of the original 453 showed diffusion (19%). Of these, 30 flicker between two vacancy states until a nearby rearrangement generally leads to the disappearance of the vacancy (of these one flickering state survives for more than 0.1 s). The remaining 56 (65%) diffuse only once and then rapidly vanish through local reorganization in their new state. Not counting the oscillations, therefore, no vacancy manages to diffuse, as a four dangling-bond cluster, for more than a single step. Two types of diffusive motions are observed for the vacancies that survive their single jump. The first one, which occurred for 74 of the diffusing vacancies, can be characterized as a first-neighbor diffusion where the vacancy at the initial and final positions share at least one threefold coordinated atom. The average distance between the

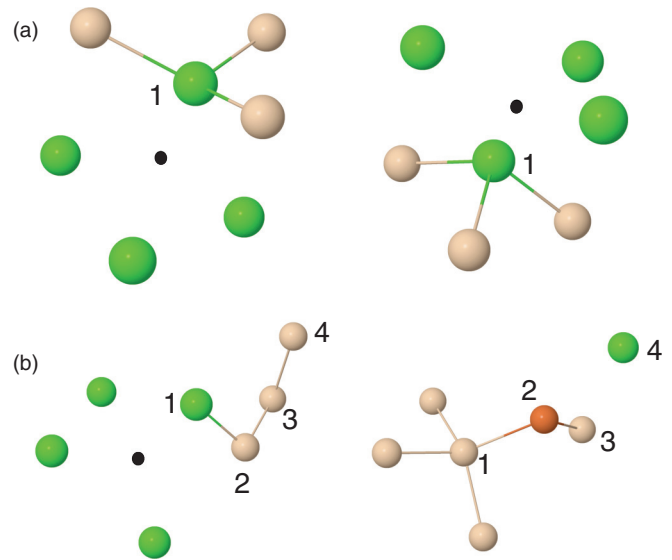


FIG. 4. (Color online) (a) Initial and final configurations of a typical vacancy diffusion event. (b) Initial and final configurations of a typical vacancy annihilation event. Green (peach, orange) atoms are threefold (fourfold and fivefold) coordinated. Small black dots indicate the center of the vacancy. See text for details.

two vacancy centers in this case is 1.75 \AA . Figure 4(a) shows the neighbor exchange necessary for this diffusive motion. The other type of motion, observed in 18 cases, is associated with a second-neighbor atom. Here, the four threefold atoms rearrange into a fully coordinated configuration pulling on their neighbors, which opens a hole created at a typical distance of 4.4 \AA . This second-neighbor diffusion typically occurs in a few steps: the initial vacancy first is partially reconstructed, with the remaining defects diffusing and flickering until a fully formed vacancy appears at the new position. In all cases, the new vacancies are destroyed immediately after being formed, with a significant energy release.

Most annihilation events are very similar: one of the four threefold atoms surrounding the vacancy moves in, bonding with the other three threefold atoms while keeping a bond with only one of its current neighbors. This neighbor in turn usually moves with the defective atom, bonding with the two threefold neighbors left behind [see Fig. 4(b)]. In some cases, a third atom is also dragged along with the first two in a chainlike motion, again exchanging neighbors as in this example. This chain is usually characterized with either the final atom breaking a single bond and leaving an isolated threefold coordinated defect or with the final atom making a long bond, near cutoff, with a nearby neighbor. Full annihilation events featuring no new coordination defect creation accounted only for 48 cases. In general, a dangling or a floating bond remains, either at the vacancy site or nearby. More precisely, 257 of the 447 (57%) annihilation events removed all four of the vacancy's dangling bonds at once. Of these, 180 events saw the creation of at least one new threefold coordinated atom. Floating bond creation is more uncommon (110 times) and usually associated with the simultaneous creation of a dangling bond (81 times). Partial annihilation events where only 3, 2, or only 1 of the dangling bonds forming the vacancies were removed, were seen 110 (25%), 76 (17%)

and 4 (<1%) times respectively. It is worth noting that these remaining defects are often short lived. For some vacancies, a previous event is needed to bring the defective atoms closer together before the actual annihilation can occur. For instance, two of the defective atoms can form a strained bond, bringing one of them close enough to the other two defects so as to reduce the activation barrier needed for the final annihilation event (vac 572).

IV. DISCUSSION

Our results all point to the observation that in *a*-Si, isolated coordination defects are more stable and can diffuse more readily than full vacancies. Indeed, we see that the *a*-Si network is surprisingly flexible and that it does not tend toward point defect clustering. Moreover, unlike with the vacancy-interstitial pair in *c*-Si, vacancy annihilation in *a*-Si does not require the presence of an opposite high-density defect to take place. Recently,³⁵ Roorda *et al.* described structural relaxation in *a*-Si as a process of vacancylike defect annihilation. The structure of the material is described as a continuous random network under compressive stress in which vacancylike defects are present. Annihilation of the vacancy void would then let the surrounding network expand, relaxing the tetrahedral local structure around each atom. The expansion would be offset by the densification created by the annihilation of the vacancies, keeping the average density constant. While our results do confirm that vacancy annihilation has a positive effect on the global network strain, especially when the local region surrounding the vacancy is under compressive stress, the vast majority of our vacancies annihilate too rapidly to take part in a long-time structural relaxation. Moreover, our simulations took place in a well-relaxed *a*-Si model, far from the much more unstable atomic environment these defects would find themselves in following an external perturbation such as a full ion collision cascade. The greater the local compressive stress, the easier it is for the disordered network to fill the void and relax. It is unlikely then that vacancies are the main point defect responsible for long-time structural relaxation. While they could still play some part, it is unlikely that they are the main actors. In the same way, the structural traps for fast diffusers such as Pd could also be isolated dangling bonds or the network could also respond to the impurity's presence

(i.e., strained or weakly bonded regions could more easily reorganize as stronger trap sites). The density could still be kept constant when considering homogeneously distributed pockets of high-density and low-density regions. These do not have to be made of coordination defects (although defects can be present). As we have seen, our original model, even when the average pressure was removed, showed a wide distribution of local pressures. It could be that relaxation reduces the width of this distribution without affecting the average value. Finally, although the exact empirical potential used will undoubtedly affect the precise quantitative value of the activation barriers and the lifetime of each vacancy, we believe that the network flexibility observed and the fact that the vacancies cannot diffuse without annihilating is representative of the underlying physics of the system.

V. CONCLUSION

In conclusion, the role of vacancylike defects in the long-time relaxation of *a*-Si, a model system for disordered covalent materials, was studied using the kinetic ART method. This method allows off-lattice atomistic simulations over time scale of a second or more. From our results, it seems unlikely that vacancylike defects play a major role in structural relaxation. Even when starting from a well-relaxed structure, only 0.6% of the 1000 vacancies created survived for more than 0.1 s at 300 K; none was able to diffuse, as a correlated dangling-bond cluster, more than once.

On a more general note, we have shown that k-ART is a powerful method especially capable of describing the long-time evolution of disordered structures. As such, it creates the opportunity to compare with experimental results that were out of reach of traditional computational methods.

ACKNOWLEDGMENTS

The authors thank Professor Sjoerd Roorda for useful discussions. This work was supported in part by the Canada Research Chairs program, the Natural Sciences and Engineering Research Council of Canada (NSERC), and the Fonds de recherche du Québec - Nature et Technologies (FRQNT). We are grateful to Calcul Québec (CQ) for generous allocations of computer resources.

¹S. Roorda, W. C. Sinke, J. M. Poate, D. C. Jacobson, S. Dierker, B. S. Dennis, D. J. Eaglesham, F. Spaepen, and P. Fuoss, *Phys. Rev. B* **44**, 3702 (1991).

²R. Karmouch, J.-F. Mercure, Y. Anahory, and F. Schiettekatte, *Appl. Phys. Lett.* **86**, 031912 (2005).

³J.-F. Mercure, R. Karmouch, Y. Anahory, S. Roorda, and F. Schiettekatte, *Phys. Rev. B* **71**, 134205 (2005).

⁴R. Karmouch, Y. Anahory, J.-F. Mercure, D. Bouilly, M. Chicoine, G. Bentoumi, R. Leonelli, Y. Q. Wang, and F. Schiettekatte, *Phys. Rev. B* **75**, 075304 (2007).

⁵K. Laaziri, S. Kycia, S. Roorda, M. Chicoine, J. L. Robertson, J. Wang, and S. C. Moss, *Phys. Rev. Lett.* **82**, 3460 (1999).

⁶S. Coffa, J. M. Poate, D. C. Jacobson, W. Frank, and W. Gustin, *Phys. Rev. B* **45**, 8355 (1992).

⁷S. Coffa, J. M. Poate, D. C. Jacobson, and A. Polman, *Appl. Phys. Lett.* **58**, 2916 (1991).

⁸S. Coffa and J. M. Poate, *Appl. Phys. Lett.* **63**, 1080 (1993).

⁹S. Coffa, F. Priolo, and A. Battaglia, *Phys. Rev. Lett.* **70**, 3756 (1993).

¹⁰S. Coffa, D. C. Jacobson, J. M. Poate, and F. Priolo, *Appl. Phys. A* **54**, 481 (1992).

¹¹W. Zachariasen, *J. Am. Chem. Soc.* **54**, 3841 (1932).

¹²S. Coffa and J. M. Poate, *Appl. Phys. Lett.* **59**, 2296 (1991).

- ¹³G. T. Barkema and N. Mousseau, *Phys. Rev. Lett.* **81**, 1865 (1998).
- ¹⁴R. Lutz and L. J. Lewis, *Phys. Rev. B* **47**, 9896 (1993).
- ¹⁵E. Kim and Y. H. Lee, *Phys. Rev. B* **51**, 5429 (1995).
- ¹⁶E. Kim, Y. H. Lee, C. Chen, and T. Pang, *Phys. Rev. B* **59**, 2713 (1999).
- ¹⁷C. R. Miranda, A. Antonelli, A. J. R. da Silva, and A. Fazzio, *J. Non-Cryst. Solids* **338–340**, 400 (2004).
- ¹⁸X. Urli, C. L. Dias, L. J. Lewis, and S. Roorda, *Phys. Rev. B* **77**, 155204 (2008).
- ¹⁹F. El-Mellouhi, N. Mousseau, and L. J. Lewis, *Phys. Rev. B* **78**, 153202 (2008).
- ²⁰L. K. Beland, P. Brommer, F. El-Mellouhi, J.-F. Joly, and N. Mousseau, *Phys. Rev. E* **84**, 046704 (2011).
- ²¹J.-F. Joly, L. K. Béland, P. Brommer, F. El-Mellouhi, and N. Mousseau, *J. Phys.: Conference Series* **341**, 012007 (2012).
- ²²N. Mousseau, L. K. Béland, P. Brommer, J.-F. Joly, F. El-Mellouhi, E. Machado-Charry, M.-C. Marinica, and P. Pochet, *Journal of Atomic, Molecular, and Optical Physics* **2012**, 1 (2012).
- ²³R. Malek and N. Mousseau, *Phys. Rev. E* **62**, 7723 (2000).
- ²⁴E. Machado-Charry, L. K. Béland, D. Caliste, L. Genovese, T. Deutsch, N. Mousseau, and P. Pochet, *J. Chem. Phys.* **135**, 034102 (2011).
- ²⁵F. Valiquette and N. Mousseau, *Phys. Rev. B* **68**, 125209 (2003).
- ²⁶H. Kallel, N. Mousseau, and F. Schiettekatte, *Phys. Rev. Lett.* **105**, 045503 (2010).
- ²⁷B. D. McKay, *Congr. Numer.* **30**, 45 (1981).
- ²⁸M. K. A. B. Bortz and J. L. Lebowitz, *J. Comp. Phys.* **17**, 10 (1975).
- ²⁹B. Puchala, M. L. Falk, and K. Garikipati, *J. Chem. Phys.* **132**, 134104 (2010).
- ³⁰F. Wooten, K. Winer, and D. Weaire, *Phys. Rev. Lett.* **54**, 1392 (1985).
- ³¹G. T. Barkema and N. Mousseau, *Phys. Rev. B* **62**, 4985 (2000).
- ³²R. Vink, G. Barkema, W. van der Weg, and N. Mousseau, *J. Non-Cryst. Solids* **282**, 248 (2001).
- ³³J. S. Custer, M. O. Thompson, D. C. Jacobson, J. M. Poate, S. Roorda, W. C. Sinke, and F. Spaepen, *Appl. Phys. Lett.* **64**, 437 (1994).
- ³⁴M. J. Demkowicz and A. S. Argon, *Phys. Rev. B* **72**, 245205 (2005).
- ³⁵S. Roorda, C. Martin, M. Droui, M. Chicoine, A. Kazimirov, and S. Kycia, *Phys. Rev. Lett.* **108**, 255501 (2012).